

Summer Report on the $^{26}\text{Al}(\text{p},\gamma)^{27}\text{Si}$ Reaction at DRAGON

Mike Anderson

In partial completion of the co-op program requirements

University of Victoria

TABLE OF CONTENTS

1. Introduction.....	4
2. The DRAGON Facility.....	5
3. Ion Chamber Simulations.....	6
3.1 Data.....	7
4. Beam Contamination.....	12
4.1 Calibration.....	12
5. Preliminary Results.....	14
5.1 Experimental Values.....	14
References.....	17
Appendix A: Simulation analysis code.....	18
Appendix B: Omega-gamma calculator code.....	20

List of Figures

1. DRAGON.....	5
2. Simulated Energies.....	7
3. Simulated Signals.....	8
4. Two-dimensional Signal Plots.....	9
5. Dual MCP Timing.....	10
6. MCP/PGAC Timing.....	11
7. HPGe Detector.....	12
8. NaI Detector.....	12
9. Calibration Plot.....	13
10. Elastics Data.....	15
11. Coincidence Data.....	16

1. INTRODUCTION

The $^{26}\text{Al}(p,g)^{27}\text{Si}$ reaction has begun at DRAGON, the Detector of Recoils And Gammas of Nuclear reactions. The experiment is done in inverse kinematics, meaning an aluminum ion produced and accelerated is incident on a hydrogen gas target. The resulting mix of beam ions and ^{27}Si then moves through the DRAGON, which separates the two, allowing silicon recoils to hit the end detectors.

In order to suppress the leaky beam incident of the end detectors, a coincidence measurement is made. For the $^{26}\text{Al}(p,g)$ experiment, however, further methods of suppression were examined. An ion chamber was used to aid in element separation, and local timing set-ups were examined. In order to understand these options, a number of simulations were completed. Also of importance to the experiment was an understanding of the composition of the incoming beam. Certain contaminants of mass 26 were expected to be present in the beam, notably magnesium, sodium and a metastable state of aluminum which would not react in the same way as the ground state. New hardware and analysis was required to look for these contaminants. Also, some programs were written in FORTRAN to aid with data analysis.

This reaction is of astrophysical interest as ^{26}Al decays via a characteristic gamma-ray which can be readily observed. The $^{26}\text{Al}(p,g)^{27}\text{Si}$ reaction is the only direct ^{26}Al destruction process besides β -decay. The reaction rate is currently known to within a factor of four, far from the 20% uncertainties required for consistent astrophysical modelling. Of increasing interest is the extent of ^{26}Al in explosive stellar environments, such as novae and supernovae, environments which the DRAGON facility was made to examine.

In this report, a brief overview of DRAGON will be given, then the results of the various simulations and contamination measurements, and, finally, some preliminary results from the experiment.

2. DRAGON

The DRAGON is a mass spectrometer. The major components are two magnetic and two electrostatic dipoles, along with a slew of quadrapoles, sextupoles and steering magnets.

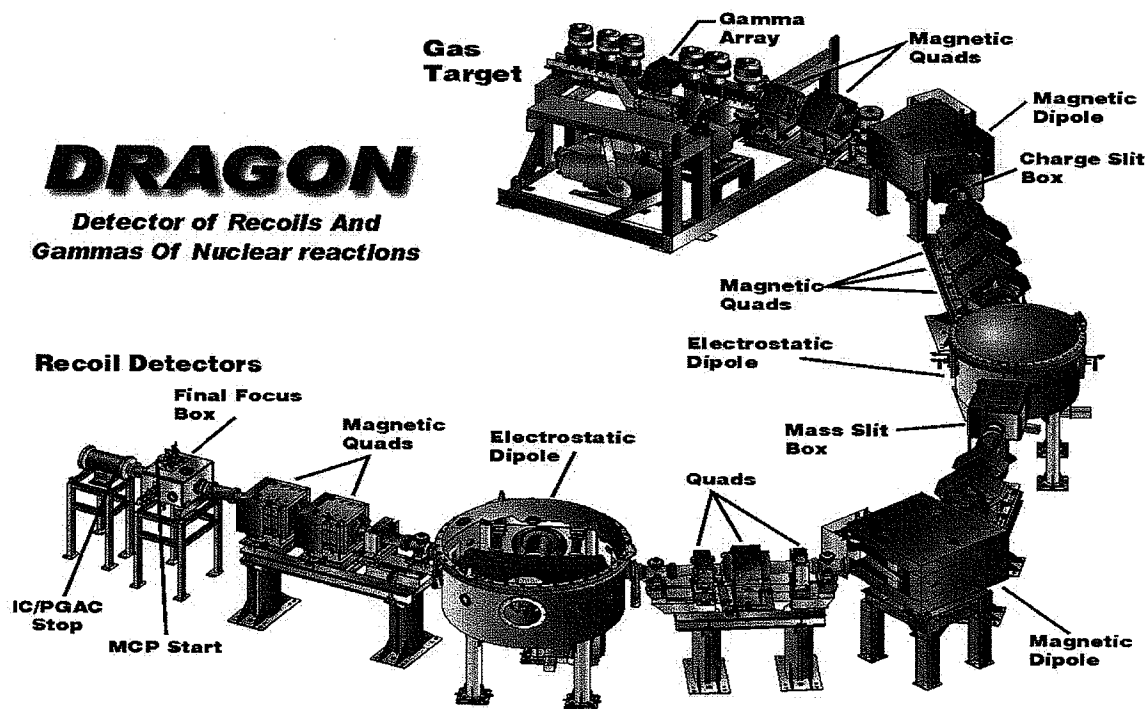


Fig.1- The standard picture of the DRAGON facility.

The gas target is surrounded by a BGO gamma detector array, which covers most of the 4-pi solid angle around the target box. The target itself is a windowless gas target, surrounded by pumping tubes to keep the rest of the beam line at good vacuum. The first magnetic dipole separates ions by charge, selecting a single charge state. Behind the dipole, there is a box containing slits, which can be opened or closed, and which physically stop the other charge states. Also in this box is a Faraday cup for measuring beam intensity. The electrostatic dipoles separate ions by energy, which becomes a de facto separation by mass. After the first electric dipole is another slit box, and after a second magnetic dipole/electrostatic dipole pair, a final slit box just in front of the ion chamber. The final slit box also contains a micro-channel plate, or MCP, which is used for timing measurements and can also display position information. The quadrapoles focus the beam, sextupoles deal with second order optics, and steering magnets aid in tuning the beam through DRAGON. For more information on the DRAGON facility, refer to Hutcheon et al., 2003.

3. ION CHAMBER SIMULATIONS

In the $^{26}\text{Al}(p,g)$ reaction, the resonance states of interest had sufficiently low strengths for the efficiency of a coincidence measurement to be a concern. Coincidence measurements at DRAGON are done using the time of flight between the BGO array and an end detector. If both detectors register a hit within a time window reflecting the amount of time an ion of the proper energy would take to transit through DRAGON, the event is recorded as a coincidence event. The BGO array, however, has an efficiency of only 40 percent in the energy region of interest for the ^{26}Al reaction, so less than half of all true recoils are recorded as coincidences. In order to preserve good statistics for very low resonance strengths, recording every good event was considered a priority. To achieve this, the DRAGON facility has both an IC, ion chamber, and PGAC, parallel grid avalanche counter. Both are housed in the same gas chamber. The IC can distinguish between different elements because each has a different stopping power. The chamber is filled with isobutane gas, with anodes every five centimeters. As the ions lose energy in the gas, secondary electrons are produced, which move under the influence of an applied electric field towards the anodes. This causes a signal to be produced in the anode which is then measured by the DRAGON electronics. By seeing where energy is deposited, the different elements could be separable.

The PGAC is not currently running, but theoretically works using the same secondary electrons to get both timing and position information. Investigating whether or not having the PGAC for local timing could give further suppression of leaky beam was also a goal of the simulations.

The simulations were done in SRIM, Stopping and Range of Ions in Matter, a free program which calculates the stopping powers of various ions in different targets. It also contains a Monte-Carlo simulator for individual ions incident on a complex target of user specification. The outputs of this program used came in the form of the energy of ions after passing through a multi-layer target of the same composition as the MCP foil, IC window, and isobutane gas. These outputs were then analysed using a FORTRAN program, and imported into PAW++, where the results could be displayed and compared with experimental values. The input ions were ^{26}Al from the beam, along with two potential contaminants, ^{26}Mg and ^{26}Na , and the recoil ion, ^{27}Si . The input energy was determined by assuming that a reaction would take place in the middle of the gas target. Then SRIM was used to find the energy of ^{27}Si after moving through half of the gas target, starting with the reaction energy. The simulated reaction was the 188 keV resonance of $^{26}\text{Al}(p,g)$.

To simulate the kinematic energy spread due to emission of a gamma ray, one energy was used for each input ion: the mean energy of silicon after the gas target, which simulates the low energy tail of the beam. This low energy tail is most likely to obscure the barrier between recoils and leaky beam. The recoils were then kinematically spread in energy in the FORTRAN analysis program using spread values from putting recoils through SRIM at the two extreme energies, corresponding to a gamma ray being emitted in the forward or backward directions. The code was also capable of spreading the data to simulate detector resolution, and this was used on the timing data. For the FORTRAN code used in analysis, see appendix A.

3.1 ION CHAMBER DATA

The direct output of the simulation was a table of energies after passing through the multi-layer target. By adding and removing layers from this target, an idea of the energy for all four elements at each point in the MCP/IC system can be gained.

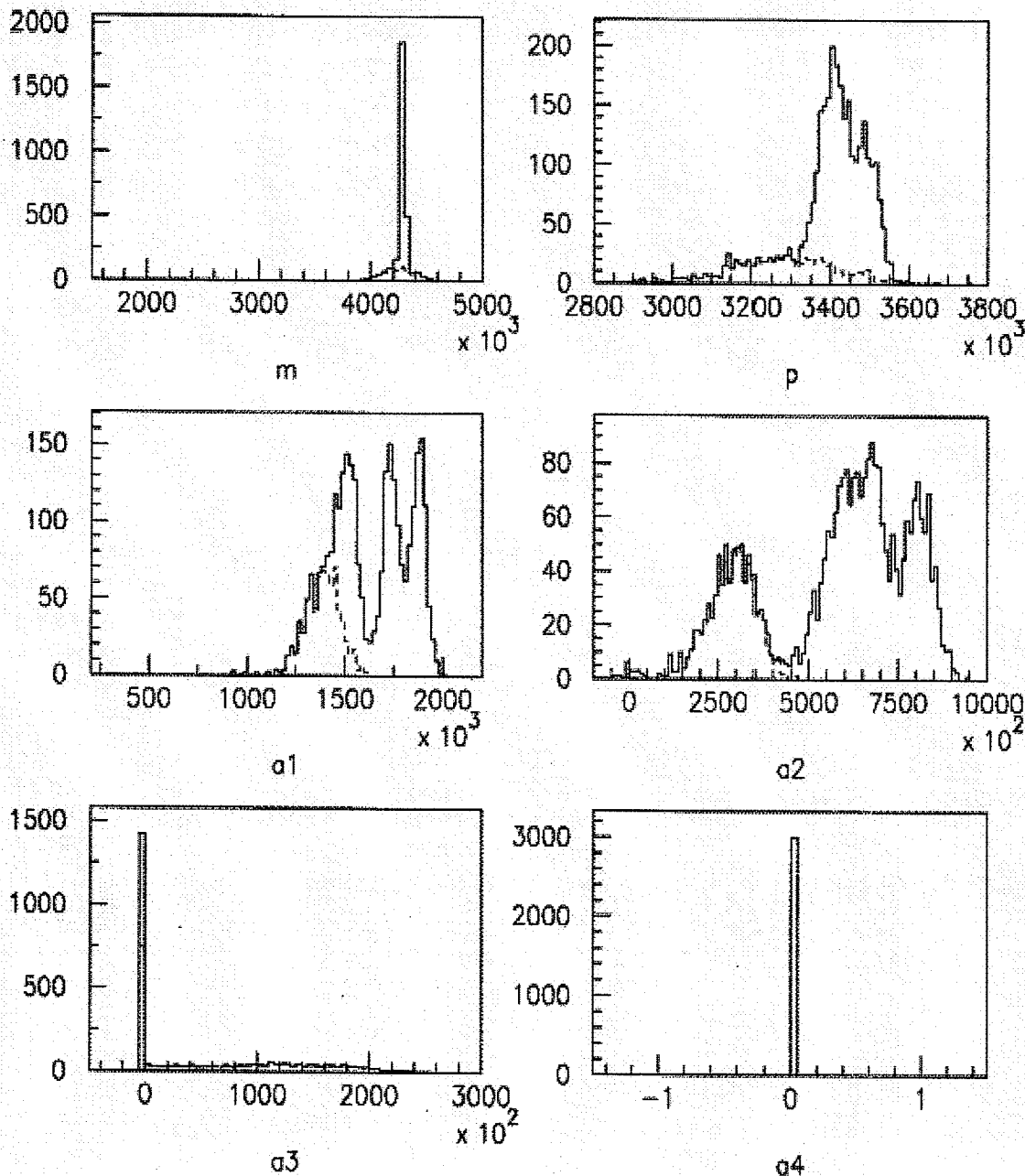


Fig 2- The energy of ions after passing through successive elements in the MCP/IC system. First the MCP foil, which is 88.77nm of carbon. Then the IC window, 600nm of polypropylene, and PGAC, 2mm of isobutane. Finally, anodes 1, 2, 3, and 4, each 5cm of isobutane. The recoil atoms are denoted by a dotted line.

The actual detected signal from the IC is not the energy of the ion, however. The IC anodes only measure energy lost across that anode, ie. The energy coming into that anode minus that going out. This subtraction was preformed in analysis. Also, signals from anodes two, three, and four were added to make a number called sigsum; this is a quantity which is already set up in the real IC electronics.

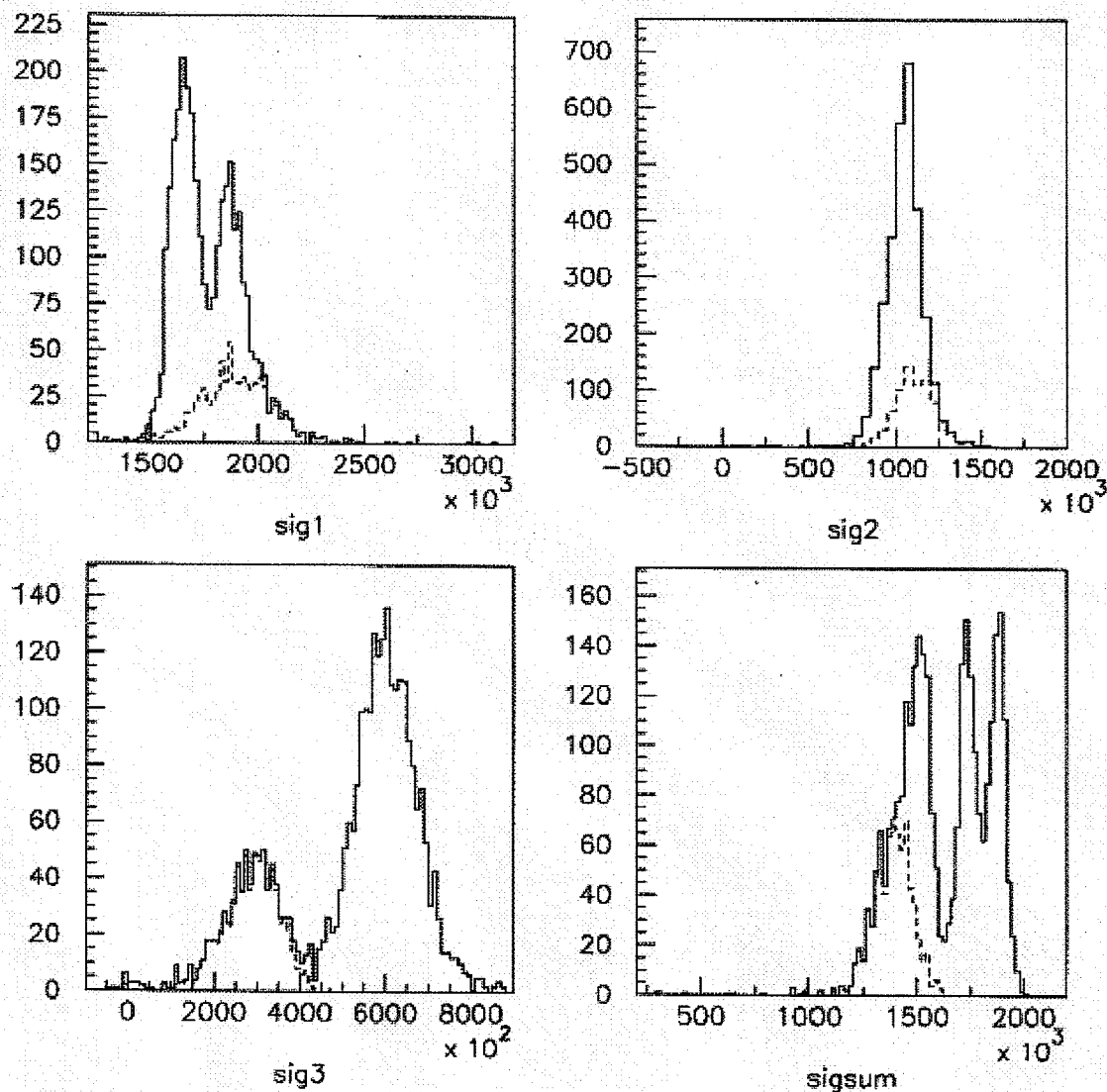


Fig 3- The signal in the first three anodes and the sum of signals from anodes two, three and four. Again, silicon is denoted by a dotted line.

PAW is capable of displaying 2 and even 3 dimensional plots. The best combination of plots to use for element identification was an objective, and depended on the input energy of the ions.

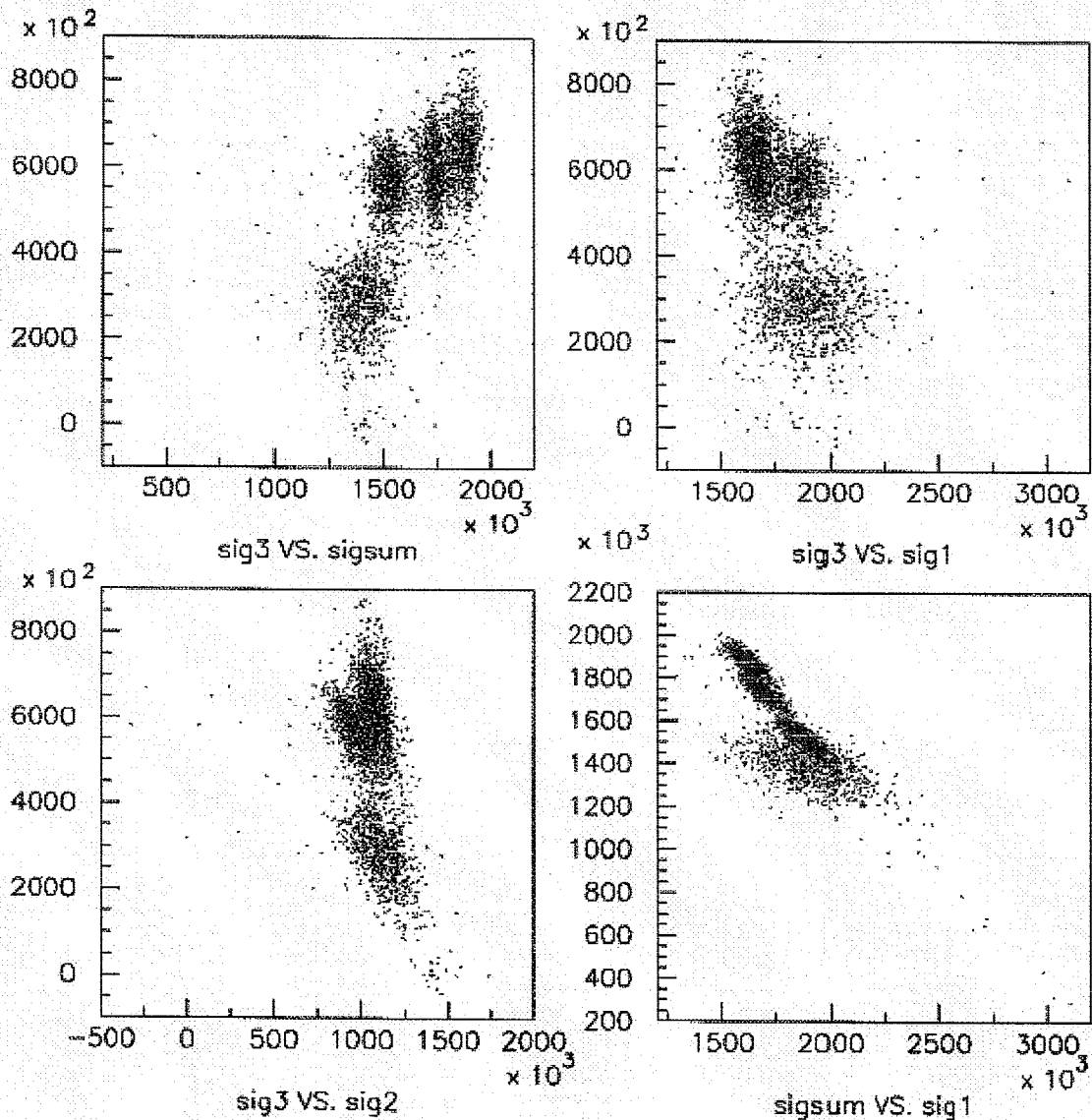


Fig 4- Two-dimensional plots of the anode signals. Anode three gives the best separation overall and was used in each case as the vertical axis. On the horizontal axis are; the sum of all three signals, anode 1 signal, and anode 2 signal. Silicon is always lower on the vertical axis.

The best separation on both axes comes from the signal on anode 3 versus sigsum, as shown above. The sigsum versus anode 1 signal plot showed no clear separation of recoils from beam.

Finally, local timing was examined. Two different systems had been proposed, a dual MCP system, and a MCP/PGAC system, which DRAGON already has all the hardware for. Both were simulated by taking the energy after the MCP foil, converting it to a velocity, and then to a time of flight using the known distance from the MCP to the next MCP, 50cm, or the IC window, 49.8cm. For the PGAC simulations, the time of flight after the IC window and 2mm of isobutane was added to this number. For each simulation, some the time resolution of the detector was taken into account. The time values were spread using a gaussian with one sigma equal to the value of the time resolution given. The MCP simulations were done with no spread, 350ps, and 700ps time resolution. For the PGAC, simulations were done with zero, 350ps, and 1200ps time resolution. These numbers reflect the resolution of a perfect system, that of the MCP alone, and that of a complete local timing system respectively. The detector resolution for an MCP comes from M. Lamey's thesis, and that for a PGAC comes from a conversation with J. Caggiano.

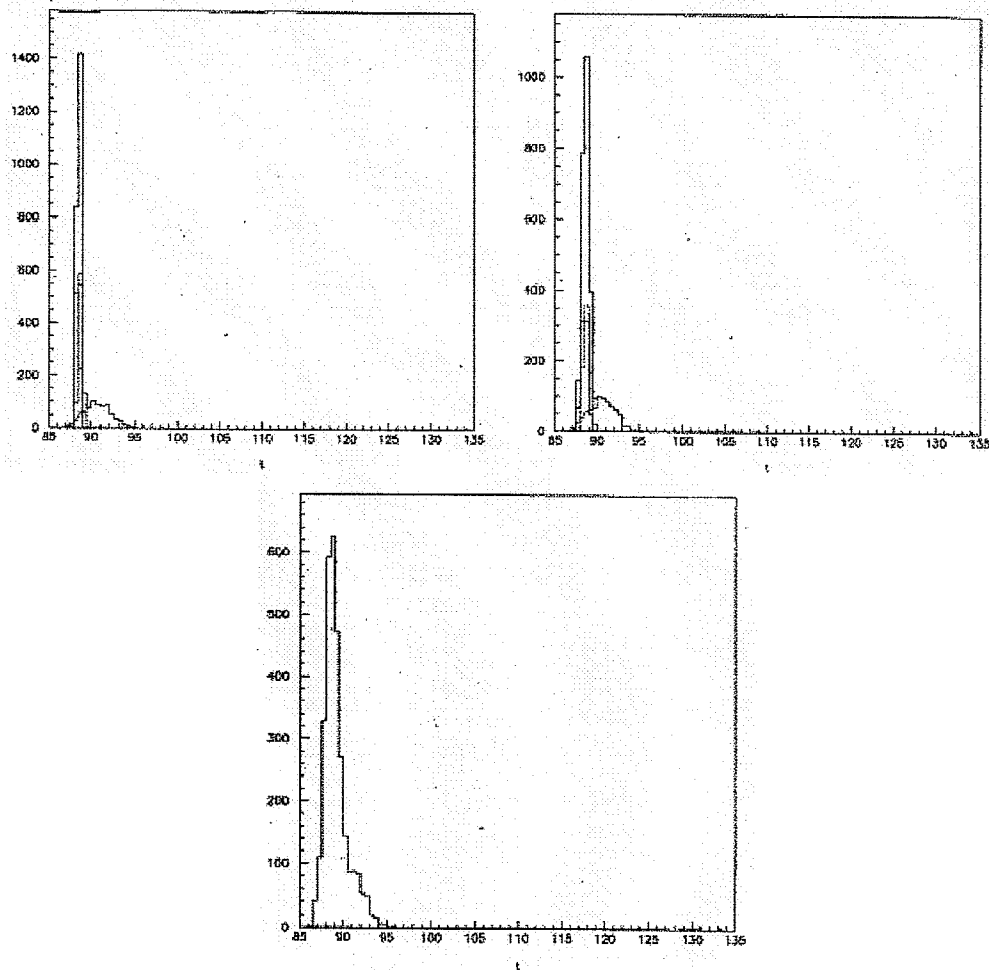


Fig 5- A dual MCP local timing system. Shown are no spread, 350ps, and 700ps detector spread respectively. The 700ps spread is a pessimistic resolution for a dual MCP system. Silicon is the low, spread out peak.

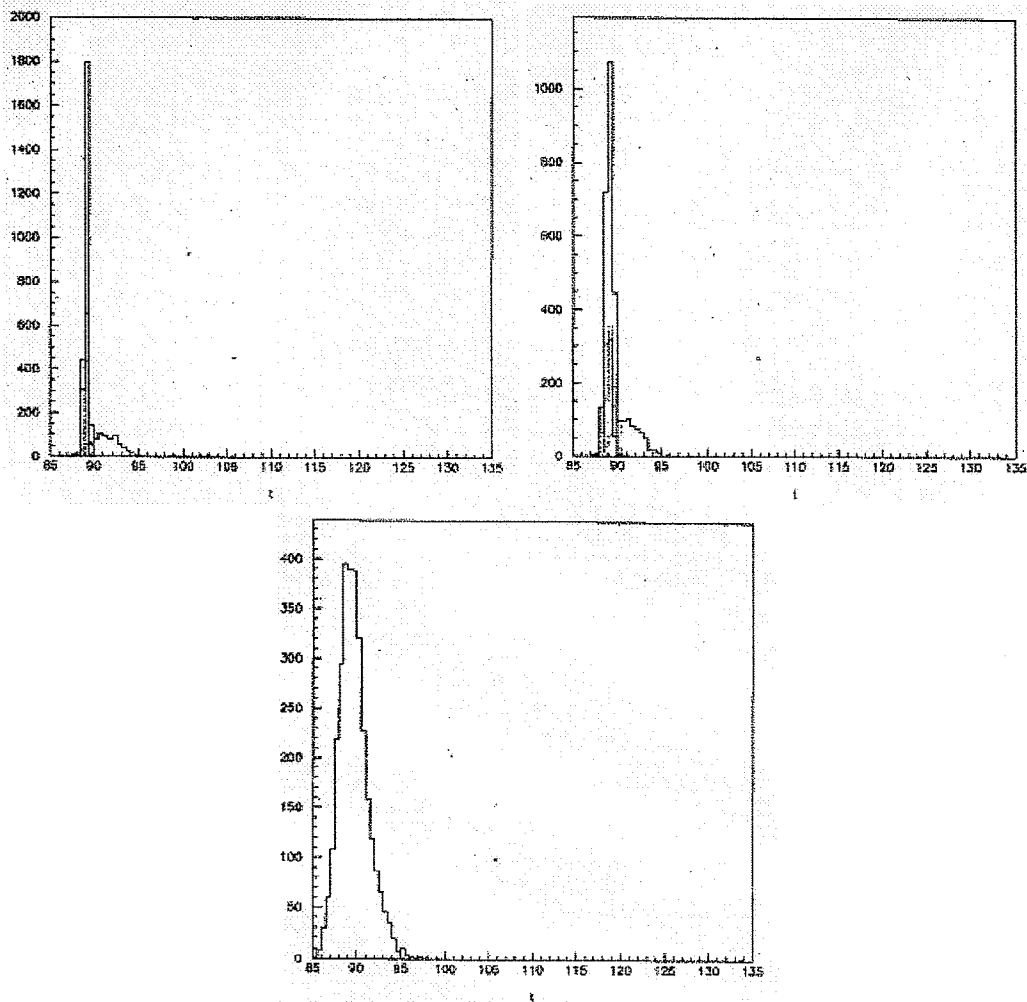


Fig 6- An MCP/PGAC timing system. Shown are no spread, 350ps, and 1200ps spread respectively. The 1200ps resolution is very reasonable for a MCP/PGAC system. Again, silicon is the low, spread out peak.

For the 188keV resonance of the $^{26}\text{Al}(p,g)$ reaction, resolution on a dual MCP system could be sufficiently reduced to make local timing a useful method of beam suppression. A PGAC system, however, does not seem to have the resolution required to make silicon recoils distinct from beam ions. Also, the IC is capable of element separation for this reaction, according to these simulations.

4. BEAM CONTAMINATION

Three major contaminants were expected in the ^{26}Al beam from ISAC. Two were observable, ^{26}Na and $^{26\text{m}}\text{Al}$, and the third not observable, ^{26}Mg .

^{26}Na decays to ^{26}Mg via beta decay along with the emission of a 1.8 MeV gamma ray. The gamma ray is easy to detect, and so to measure it a HPGe detector was placed by the mass slits. When the beam is deflected into the slits by the electrostatic dipole, it will continue to decay as usual and so gammas emitted towards the detector will be seen. This system was set up and calibrated.

$^{26\text{m}}\text{Al}$ decays directly to the ground state of ^{26}Mg via a positron emission. In order to detect this, a 'horn' was assembled on top of the mass slits, with two NaI detectors sitting opposite each other beside it. The NaI detectors were set to pickup coincidence .511 MeV gammas from the annihilation of the positron with an electron. Calibration of this device was done by A. Ruberg and K. Oraas.

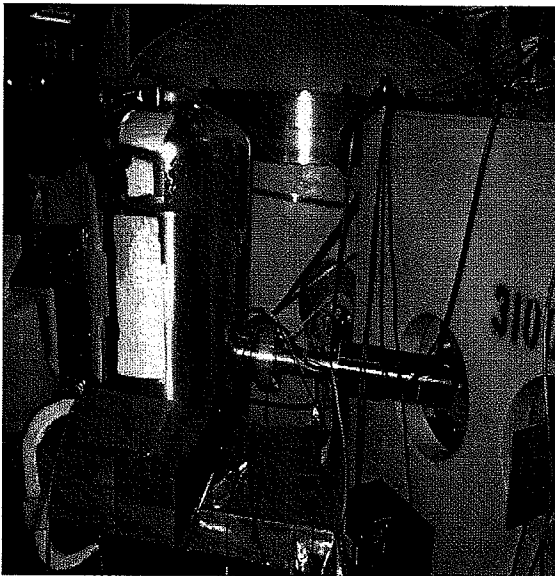


Fig 7- The HPGe detector on its stand. Also visible are the first electric dipole and the mass slit box. The detector is pointed at the beam intersection point on the mass slit.

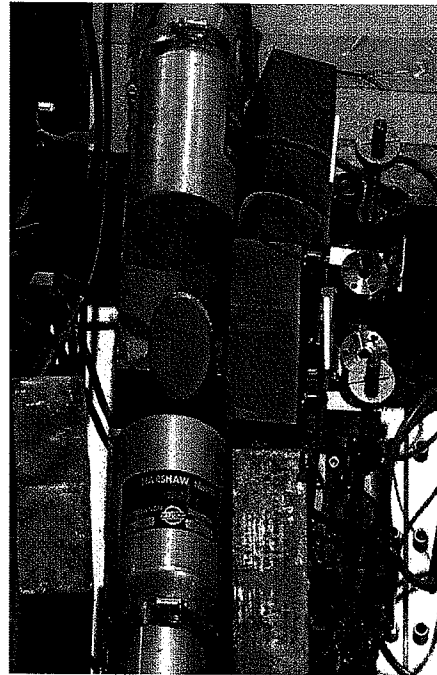


Fig 8- The two NaI detectors on either side of the 'horn', dubbed the Unicorn. The detectors are surrounded by lead bricks, to cut background.

4.1 CALIBRATION

Calibration of the HPGe detector was done using a number of radioactive sources placed on the mass slit at the position where beam would hit. The response of the detector to these known sources was then observed. By finding the detected activity of the source and comparing it to the known activity, the efficiency was calculated. Of particular value

was ^{88}Y , which emits a gamma ray at 1.83 MeV, very close to the 1.8 MeV gamma of ^{26}Na decay.

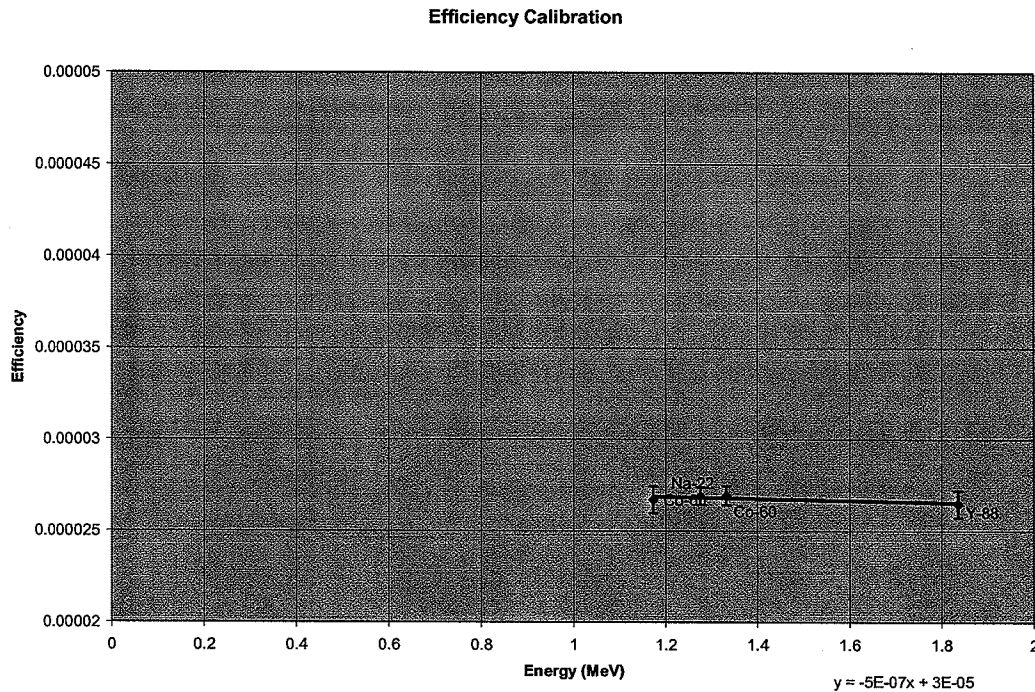


Fig 9- The energy calibration curve for the HPGe detector. The errors in this plot are statistical, from the detector software, and hover around 2%.

The current activity for each of these sources was calculated using the manufacturer's given activities and the well known half-life relation:

$$A = A_0 \cdot \exp[-t \cdot \ln(2)/t_{1/2}]$$

Where t is time since last calibration, A the current activity, A_0 the activity at time $t=0$, and $t_{1/2}$ the half-life. Half-lives were found in the table of the nuclides.

The detected activity came from a number of counts, minus background, divided by the total live time of the detector. The background subtraction, total live time, and statistical error on counts were given by the detector software. Using this method, a total efficiency of $.00265 \pm .00007$ % was obtained. A calibration of the NaI detector done by A. Ruberg and K Oraas found a total efficiency for that system of $.00227 \pm .00023$ %. Using these numbers, a computation of the beam contamination was done during some of the actual runs. The isomeric state of aluminum was found to make up $.37 \pm .07$ %, and ^{26}Na to make up $.0048 \pm .0007$ %, of the of the incoming beam. This is a negligible amount. Later observations showed that the contaminant levels were likely not constant over the length of a run.

5. CURRENT RESULTS

The $^{26}\text{Al}(p,g)^{27}\text{Si}$ reaction is ongoing at DRAGON. Runs during the summer focused on both the 188 keV and the 363 keV resonances. Because of electronics failures, coincidence measurements between the BGO and end detector had to be used. For the 363 keV resonance, data was still collected with reasonable statistics, but the 188 keV resonance failed to show even a single recoil event, even after over 100 hours of running. The lack of reactions is primarily due to the low beam intensity, and is in agreement with the expected resonance strength.

Using data from the 363 keV resonance runs, a preliminary omega-gamma was calculated. Omega-gamma is a number in units of energy, which characterises the strength of a reaction. For a derivation and description of omega-gamma, please refer to Shawn Bishop's thesis. Presented here without derivation:

$$\omega\gamma = 2 * Y * \epsilon * m_2 / (\lambda^2 * (m_1 + m_2))$$

Where Y is the reaction yield, ϵ the stopping power of the beam ion in the gas target, λ the de Broglie wavelength, and m_1 and m_2 the masses of the beam and target ions, respectively. The reaction yield is an interesting calculation in itself, which includes a number of systematic effects of the DRAGON facility. For this calculation, Y was taken to be:

$$Y = N_d / (N_i * \text{CSF} * G_{\text{eff}} * \text{LIVE})$$

Where N_d is the number of detected recoils, N_i is the number of incident beam particles, CSF is the charge state fraction of the selected charge state, G_{eff} is the efficiency of the BGO gamma array, and LIVE is the live time of the DRAGON end detectors.

The omega-gamma was calculated using another small FORTRAN program, which can be seen in appendix B.

5.1 EXPERIMENTAL VALUES

Each of these numbers had to be found from simulations, experimental results, and calculations. The masses were found in tables, and λ calculated from fundamental constants and these masses, along with the resonance energy. SRIM was used to find ϵ . The BGO efficiency was found in D. Gigliotti's upcoming thesis, and the charge state fraction calculated using theory expressed in W. Liu's thesis.

The live time, number of detected recoils, and number of incoming particles were all experimentally determined. The end detectors record an event even when the data acquisition system is unable to record the specifics, and these events are recorded as HI_presented. Another number, HI_acquired, has an event counted in it if the DAQ is able to record all of the event data. By dividing HI_acquired by HI_presented, the life time is obtained as a fraction of total time.

The number of incoming particles were much more difficult to determine. Two different methods were used. The first involved using the DRAGON beta monitor, a silicon detector located opposite the mass slit. This detector would pick up the beta decay

of the beam contaminants after they are stopped on the slit. Using a Faraday cup measurement taken at the beginning of the run, a calibration of the beta monitor was performed, which allowed an integration of the beta monitor counts over the run to be converted into the number of incoming beam particles:

$$N_i = \text{Integration} * \text{FC} / (\text{Initial} * \text{CS} * 1.6\text{E-19})$$

Where Integration is the total integrated number of counts from the beta monitor over the entire run time, FC is the initial Faraday cup measurement in amps, Initial is the first count reading of the beta monitor immediately after removing the Faraday cup, and CS is the charge state of the beam, to convert from electro-amps to particle-amps. In this case, the Faraday cup used was FC4, a cup upstream of the gas target. The charge state of the incoming beam was 6+. Using this data, N_i was determined to be around $9.43 * 10^{11}$ particles. This, however, gave a wildly different omega-gamma than the previously published value. The above method rests on the assumption that the beam contaminant levels are constant, which is not necessarily true.

A second method was tried. DRAGON also has two elastics monitors inside the gas target, which detect Rutherford scattered target atoms. Using a program which simulates Rutherford scattering written by D. Hutcheon, an efficiency for the elastics detector was calculated to be 2.597E-8 . Unfortunately, no systematic errors are included with this number from the program. But using this efficiency with the number of detected events from the elastics monitors, minus noise rejected by comparing energy, N_i was found to be $(5.37 \pm 0.05) * 10^{12}$. The primary source of errors in this number is some unexplained spiking in the elastics data. The total area of the spikes was subtracted from the integration and taken as an error.

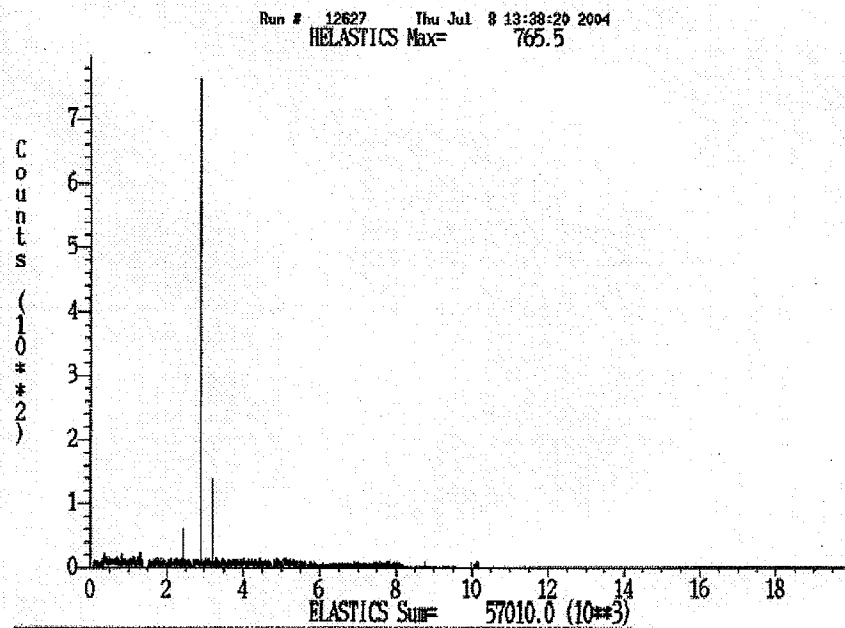


Fig 10- The elastics data used to find the number of incoming particles, showing large spikes which were the major contributor to error.

The final number, N_d , is the crucial one. The number of detected particles was determined for the 363 keV using coincidence data, due to some electronics problems in the ion chamber. The coincidence data could be looked at in a two dimensional plot showing both energy and timing with respect to the RF pulse. This allowed good rejection of noise and random coincidences, and because the 363 keV resonance is strong enough, measurements could be made with reasonable statistics using this method.

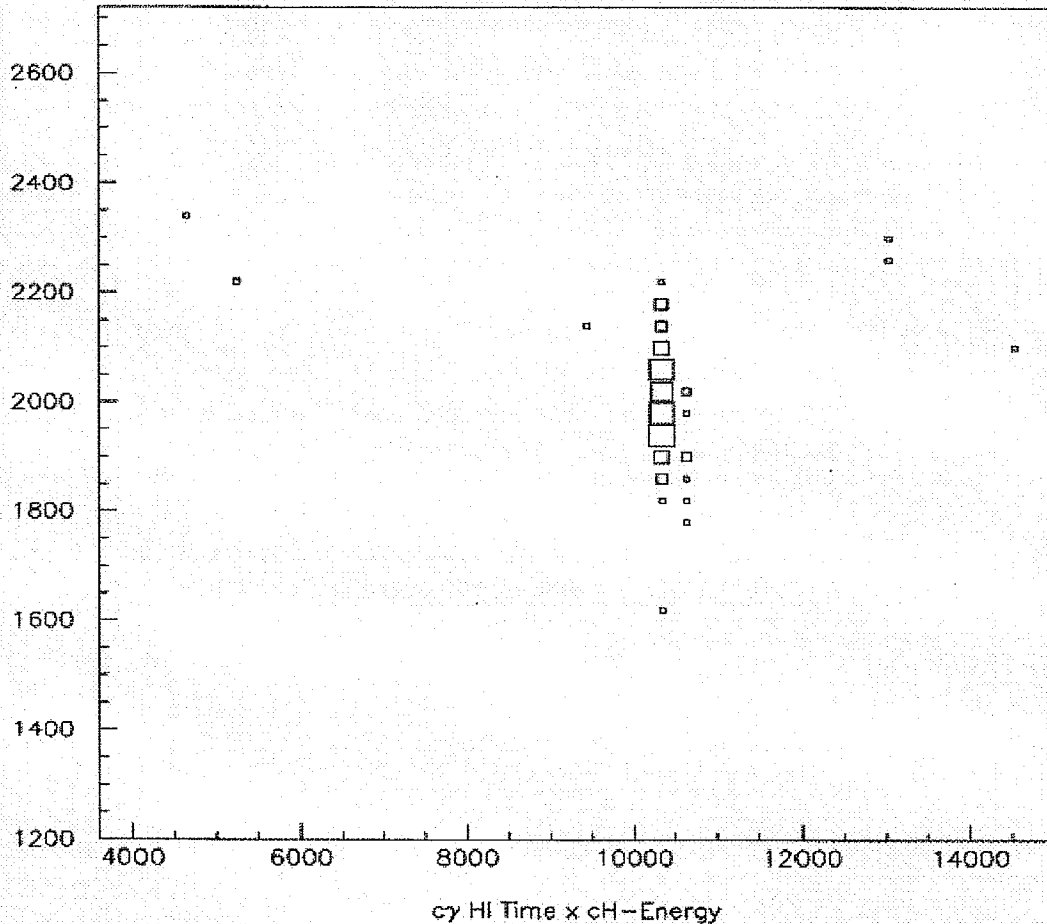


Fig 11- The PAW 2-dimensional histogram used to select recoil events in the coincidence data. The cluster of events is recoils, and all other boxes are random coincidences. Noise has already been rejected in this picture, as it simply lies at a lower energy. The vertical axis is energy, and the horizontal axis is time from the last RF pulse.

From this plot with the required rejections, N_d was found to be 110 ± 11 . The error on this number is almost entirely statistical, plus one event for the systematics of the rejection process, because a random coincidence could easily lie within the RF time window.

Using these numbers with the FORTRAN program, the omega-gamma was found to be 57 ± 15 meV. This agrees well with the previously published value by L. Buchmann of 65.

Data was collected for the 188 keV resonance of the $^{26}\text{Al}(p,g)$ reaction, but was not conclusive. The experiment is ongoing at DRAGON, with a focus on getting a higher beam intensity incident on the target in order to observe some recoils.

REFERENCES:

D.A. Hutcheon et al.; Nuclear Instruments and Methods in Physics Research A, 498, p. 190-210, (2003)

Shawn Bishop, *Direct Measurement of the $^{21}\text{Na}(p,g)^{22}\text{Mg}$ Resonant Reaction in Nova Nucleosynthesis*; Ph.D. Thesis, Simon Fraser University, (2003)

Wenjie Liu, *Charge State Studies of Heavy Ions Passing Through Gas*; M.Sc. Thesis, Simon Fraser University, (2001)

Dario Gigliotti, *Effeciency Calibration Through GEANT Simulation for the DRAGON Gamma Array at TRIUMF*; expected M.Sc. Thesis, University of Northern British Colombia, (2004)

L. Buchmann et al.; Nuc. Phys. A, 498, p.93-113, (1984)

C. Ruiz, *Astrophysical studies using ^{26}Al ground-state and isomeric beams*; TRIUMF Research Proposal E989, (2004)

Mike Lamey, *A Microchannel Detection System for DRAGON*; M.Sc. Thesis, Simon Fraser University, (2004)

Jac Caggiano, personal conversation, (2004)

Appendix A

c-----67-----

```
implicit none
real a4(4),a3(4),a2(4),a1(4),P(4),M(4),T(4),pi
real sig4(4),sig3(4),sig2(4),sig1(4),sigsum(4)
common /HEAD/ a4,a3,a2,a1,P,M,T,sig4,sig3,sig2,sig1,sigsum
real gauss
external gauss
real spread4,spread3,spread2,spread1,spreadP,spreadM
real spreadt,HRNDM1
integer Hsize,istat,icycle,i
parameter (Hsize=5e6,pi=3.1415927)
real H(Hsize)
common /PAWC/ H
call hlimit(Hsize)
call hropen(22,'dir','testb.ntp','N',1024,istat)
call hbnt(1,'testb.ntp',' ')
call hbname(1,'HEAD',a4,'a4(4):R,a3(4):R,a2(4):R,a1(4):R, '//
+          'P(4):R,M(4):R, '//
+          'T(4):R,sig4(4):R,sig3(4):R, '//
+          'sig2(4):R,sig1(4):R, '//
+          'sigsum(4):R')
open(10,file='sione.txt',status='old')
open(20,file='alone.txt',status='old')
open(30,file='mgone.txt',status='old')
open(40,file='naone.txt',status='old')
```

- c The energy spreads are from the decay, simultating a
c gamma flying off in some direction. It's not perfect.

```
spread4 = 0 !! anode4 energy spread... in ev
spread3 = 0 !! anode3 energy spread... in ev
spread2 = 37766 !! anode2 energy spread... in ev
spread1 = 70759 !! anode1 energy spread... in ev
spreadP = 130369 !! PGAC energy spread... in ev
spreadM = 139157 !! MCP energy spread... in ev
spreadT = 1.2 !! 0 ns... from detector uncertainty
```

```
call hbfun1(1000,'Gauss_spread',100,-3.0,3.0,gauss)
```

```
do i = 1, 999
```

```
  read(10,*,end=99) a4(1),a3(1),a2(1),a1(1),P(1),M(1)
99  read(20,*,end=100) a4(2),a3(2),a2(2),a1(2),P(2),M(2)
100 read(30,*,end=101) a4(3),a3(3),a2(3),a1(3),P(3),M(3)
101 read(40,*,end=999) a4(4),a3(4),a2(4),a1(4),P(4),M(4)
```

```
  a4(1) = a4(1) + hrndm1(1000)*spread4
  a3(1) = a3(1) + hrndm1(1000)*spread3
  a2(1) = a2(1) + hrndm1(1000)*spread2
  a1(1) = a1(1) + hrndm1(1000)*spread1
  P(1) = P(1) + hrndm1(1000)*spreadP
  M(1) = M(1) + hrndm1(1000)*spreadM
  sig4(1) = a3(1) - a4(1)
  sig4(2) = a3(2) - a4(2)
```

```

sig4(3) = a3(3) - a4(3)
sig4(4) = a3(4) - a4(4)
sig3(1) = a2(1) - a3(1)
sig3(2) = a2(2) - a3(2)
sig3(3) = a2(3) - a3(3)
sig3(4) = a2(4) - a3(4)
sig2(1) = a1(1) - a2(1)
sig2(2) = a1(2) - a2(2)
sig2(3) = a1(3) - a2(3)
sig2(4) = a1(4) - a2(4)
sig1(1) = P(1) - a1(1)
sig1(2) = P(2) - a1(2)
sig1(3) = P(3) - a1(3)
sig1(4) = P(4) - a1(4)
sigsum(1) = sig2(1) + sig3(1) + sig4(1)
sigsum(2) = sig2(2) + sig3(2) + sig4(2)
sigsum(3) = sig2(3) + sig3(3) + sig4(3)
sigsum(4) = sig2(4) + sig3(4) + sig4(4)

```

- c The obscure numbers at the end are the mass in ev
- c divided by 2, then sqrt'd and multiplied by 1/c in
- c cm/ns. 49.8 and 0.2 are the distances
- c in cm from the MCP to the IC and into the PGAC,
- c respectively.

```

T(1) = (sqrt(1/M(1))*49.8+sqrt(1/P(1)*0.2))*3739.635383
T(2) = (sqrt(1/M(2))*49.8+sqrt(1/P(2)*0.2))*3669.707913
T(3) = (sqrt(1/M(3))*49.8+sqrt(1/P(3)*0.2))*3669.404378
T(4) = (sqrt(1/M(4))*49.8+sqrt(1/P(4)*0.2))*3670.11329

```

```

T(1) = T(1) + HRNDM1(1000)*spreadT
T(2) = T(2) + HRNDM1(1000)*spreadT
T(3) = T(3) + HRNDM1(1000)*spreadT
T(4) = T(4) + HRNDM1(1000)*spreadT
call hfnt(1)
enddo

```

```

999 continue
call hcdir('//dir',"")
call hrout(0,icycle,"")
call hrend('dir')
end

```

c---67---

```

c Gaussian function
real function gauss(X)
real X,sigma,pi
pi = 3.1415926
sigma = 1.0
gauss = 1./ ( sigma * sqrt(2.* pi) )
gauss = gauss * exp( -X**2/(2 * sigma**2) )
return
end

```

Appendix B

```
REAL NDET,NINC,CSF,GEFF,ECM,M1,M2,EPS,OMEGAM,LIVE
REAL DNDDET,DNINC,DCSF,DGEFF,DEPS,DOMEGAM,DLIVE
REAL h,MU,LAM2,Y,DY
```

```
h = 4.1357E-21 !! in MeV*s
```

```
GEFF = .4
```

```
DGEFF = 0.01
```

```
CSF = .38
```

```
DCSF = .045
```

```
M1 = 25.98689169 !! in amu, for Al-26
```

```
M2 = 1.00794 !! in amu, for H
```

```
EPS = 1.24E-10 !! from SRIM, in mev/atom/cm2
```

```
DEPS = 0.003E-10
```

```
ECM = .363
```

```
LIVE = .93681
```

```
DLIVE = 0.0003
```

```
PRINT *, '*****MIKES OMEGA*GAMMA CALCULATOR***** '
```

```
PRINT *, ' You will need to know everything about the '
```

```
PRINT *, 'reaction. Input errors when prompted, separated by '
```

```
PRINT *, ' a comma; if there is negligible error, please '
```

```
PRINT *, ' input a zero. '
```

```
PRINT *, ' This assumes a BGO efficiency of .4 +/- .01 '
```

```
PRINT *, '*****'
```

```
c PRINT *, 'Input beam mass: (in amu)'
```

```
c READ *, M1
```

```
c PRINT *, 'Input target mass: (in amu)'
```

```
c READ *, M2
```

```
c PRINT *, 'Input center of mass energy: (in MeV)'
```

```
c READ *, ECM
```

```
c PRINT *, 'Input charge state fraction, and error: '
```

```
c READ *, CSF, DCSF
```

```
c PRINT *, 'Input live time, and error: '
```

```
c READ *, LIVE, DLIVE
```

```
c PRINT *, 'Input stopping power, and error: (in meV/atom/cm2)'
```

```
c READ *, EPS, DEPS
```

```
PRINT *, 'Input number of detected particles, and error: '
```

```
READ *, NDET, DNDDET
```

```
PRINT *, 'Input number of incident particles, and error: '
```

```
READ *, NINC, DNINC
```

```
MU = (M1*M2)/(M1 + M2)
```

```
LAM2 = (h**2*8.99e20/931.494)/(2*MU*ECM)
```

```
Y = NDET/(NINC*CSF*GEFF*LIVE)
```

```
DY = (DNDDET/NDET+DNINC/NINC+DCSF/CSF+DGEFF/GEFF+DLIVE/LIVE)
```

```
DY = DY*Y
```

```
OMEGAM = 2*Y*EPS/(LAM2*(M1+M2)/M2) !! in meV
```

```
DOMEGAM = (DY/Y+DEPS/EPS)*OMEGAM
```

```
PRINT *, 'YOUR OMEGA*GAMMA IS:', OMEGAM, ' +/- ', DOMEGAM, ' meV'
```

```
END
```